Published in final edited form as:
J Am Chem Soc. 2010 May 26; 132(20): 7049–7054. doi:10.1021/ja910583y.

The divalent metal ion in the active site of uteroferrin modulates substrate binding and catalysis

Nataša Mitić[a], **Kieran S. Hadler**[a], **Lawrence R Gahan**[a], **Alvan C. Hengge**[b,*], and **Gerhard Schenk**[a,*]

[a]School of Chemistry and Molecular Biosciences, The University of Queensland, St Lucia, Queensland, 4072, Australia

[b]Department of Chemistry and Biochemistry, Utah State University, Logan, UT, 84322-0300, USA

Abstract

The purple acid phosphatases (PAP) are binuclear metallohydrolases that catalyze the hydrolysis of a broad range of phosphomonoester substrates. The mode of substrate binding during catalysis and the identity of the nucleophile is subject to debate. Here, we used native Fe^{3+}-Fe^{2+} pig PAP (uteroferrin; Uf) and its Fe^{3+}-Mn^{2+} derivative to investigate the effect of metal ion substitution on the mechanism of catalysis. Replacement of the Fe^{2+} by Mn^{2+} lowers the reactivity of Uf. However, using stopped-flow measurements it could be shown that this replacement facilitates approximately a ten-fold faster reaction between both substrate and inorganic phosphate with the chromophoric Fe^{3+} site. These data also indicate that in both metal forms of Uf, phenyl phosphate hydrolysis occurs faster than formation of a μ-1,3 phosphate complex. The slower rate of interaction between substrate and the Fe^{3+} site relative to catalysis suggests that the substrate is hydrolyzed while coordinated only to the divalent metal ion. The likely nucleophile is a water molecule in the second coordination sphere, activated by a hydroxide terminally coordinated to Fe^{3+}. The faster rates of interaction with the Fe^{3+} site in the Fe^{3+}-Mn^{2+} derivative than the native Fe^{3+}-Fe^{2+} form are likely mediated via a hydrogen bond network connecting the first and second coordination spheres, and illustrate how the selection of metal ions may be important in fine-tuning the function of this enzyme.

1. Introduction

Purple acid phosphatases (PAPs) belong to the family of binuclear metallohydrolases and hydrolyze mono- and some diester substrates at acidic to neutral pH.[1-4] PAPs require heterovalent Fe^{3+}-M^{2+} centers (M = Fe, Zn, Mn) for catalysis, and their characteristic purple color is due to a charge transfer (CT) interaction between a conserved tyrosine ligand and the Fe^{3+} in the active site. The biological functions of PAPs are diverse and include phosphate acquisition and reactive oxygen species metabolism in plants, and bacterial killing and bone resorption in animals.[3,5,6]

In the proposed mechanistic model of the PAP-catalyzed reaction the substrate initially associates with the enzyme forming a catalytically non-competent complex.[3,4,7-11] Subsequently, rearrangements within the active site lead to the formation of a Michaelis complex where the oxygen atom of the phosphate group of the substrate is monodentately coordinated to the divalent metal ion. A number of aspects of the subsequent reaction sequence are uncertain. While the next step in the catalytic cycle involves a nucleophilic attack by a

*Addresses for correspondence: Assoc. Prof. Gerhard Schenk, School of Chemistry & Molecular Biosciences, University of Queensland, St Lucia, Queensland, 4072, Australia, schenk@uq.edu.au; Prof. Alvan C. Hengge, Department of Chemistry & Biochemistry, Utah State University, Logan, UT, 84322-0300, USA, alvan.hengge@usu.edu.

hydroxide, the identity of the nucleophile has been proposed to depend on the type of substrate and the metal ion composition in the active site.[11] The nucleophilic hydroxide has been proposed to be either: (i) terminally bound to Fe^{3+}; (ii) bridging the two metal ions; or (iii) residing in the second coordination sphere (Figure 1).[3,4,7-11] The mode of substrate binding in the Michaelis complex is also uncertain. Both M^{2+} monodentate and μ-1,3 bidentate coordination have been suggested based on a range of crystallographic, spectroscopic and kinetic studies.[3,4,7-13]

The nucleophile used in the reaction and the orientation of the substrate are likely to be associated, *i.e.* the identity of the nucleophile in the PAP-catalyzed reaction depends upon the mode of substrate binding. For instance, for a metal ion-bridging nucleophile the optimal alignment with the substrate is reached when the latter binds in μ-1,3 bidentate coordination to the active site.[12-14] If substrate reacts while bound only to the divalent metal ion, a hydroxide either terminally bound to Fe^{3+} or in the second coordination sphere are more likely candidate nucleophiles (Figure 1).

In order to probe the mode of substrate binding to PAP, and the effect of the metal ion composition thereof, we have used the PAP enzyme from pig (also known as uteroferrin; Uf) and employed stopped-flow measurements to monitor the CT interaction with inorganic phosphate and with phenyl phosphate, in two different metal ion derivatives, the native Fe^{3+}-Fe^{2+} and the Fe^{3+}-Mn^{2+} forms.

2. Materials and Methods

Materials

All chemicals used were of analytical grade and were purchased from Sigma unless otherwise stated.

Enzyme Purification

Pig PAP (uteroferrin; Uf) was isolated from the uterine fluid as described previously.[15] In brief, Uf was extracted from the uterine fluid of a pregnant sow; an initial ion-exchange chromatography step using CM-cellulose resin was followed by gel filtration on a Sephadex G-75 column. Purified Uf was stored at −20 °C in 100 mM acetate buffer at pH 4.9 until further use. The protein concentration was determined by measuring the absorbance at 280 nm using the specific extinction of 1.41 for a 1 mg/mL solution (28.6 μM) of Uf.

Metal Ion Replacement

In order to replace Fe^{2+} in the active site of Uf by Mn^{2+} 500 μL of the enzyme (7 mg; 0.1 M acetate buffer, pH 4.9) were mixed with 1 mL 30 mM 1,10-phenanthroline (in 0.1 M acetate buffer, pH 4.9) and 500 μL 100 mM sodium dithionite (freshly prepared in 0.1 M acetate buffer, pH 4.9 immediately prior to use) and incubated at room temperature for 1 min. Subsequently, the mixture was applied to a Bio-Rad Econo-Pac 10DG column (preequilibrated with 0.1 M acetate buffer, pH 4.9). The metal ion content and the activity of the half-apoenzyme was determined by atomic absorption spectroscopy (AAS) and a standard activity assay (see below), respectively. For various samples of half-apo Uf the iron content varied between 0.89 and 1.06 per active site, with only trace amounts of Zn and Cu detectable. The residual activity never reached values higher than 8 U/mg (less than 3% of the fully active holoenzyme).

To the half-apo enzyme 100 equivalents of Mn^{2+} ($MnSO_4$) were added and the activity was monitored until maximum activity was reached. The excess of Mn^{2+} was then removed by dialysis and the content of bound Mn^{2+} measured by AAS (0.87 ± 0.05).

Activity Assay

A standard continuous assay was used to determine steady state kinetic constants for Uf with phenyl phosphate (PP) or *para*-nitrophenol phosphate (*p*NPP) as substrate as described elsewhere.[16] Assays were carried out at pH 4.9 using 100 mM acetate buffer. Product formation (P or *p*NP) was monitored at 278 nm and 390 nm, respectively, using appropriate extinction coefficients (770 $M^{-1}cm^{-1}$ and 342.9 $M^{-1}cm^{-1}$).[11,16] Substrate concentrations ranged from ~0.2 x K_m to ~8 x K_m. Assay mixtures were incubated at 25°C for 5 minutes prior to the addition of enzyme (20 nM). Data displayed saturation type behavior (Michaelis-Menten behavior) and kinetic parameters were determined by fitting to equation 1 using WinCurveFit (Kevin Raner software):

$$v = \frac{V_{max} \times [S]}{K_m + [S]} \quad (1)$$

Here, v is the initial rate, [S] is the substrate concentration, V_{max} is k_{cat} multiplied by the amount of enzyme present, and K_m is the Michaelis constant.

pH Dependence Studies

Activity assays with *p*NPP and PP as substrate were carried out at 11 pH values between pH 3 and pH 7.5 using 100 mM glycine, acetate or 2-morpholinoethanesulfonic acid buffers, respectively. The k_{cat} and k_{cat}/K_m versus pH data were fit to the following equations using WinCurveFit:

$$k_{cat} = \frac{(k_{cat})^{max}}{(1 + [H]/Kes_1 + Kes_2/[H])} \quad (2)$$

$$k_{cat}/K_m = \frac{(k_{cat}/K_m)^{max}}{(1 + [H]/Ke_1 + Ke_2/[H])} \quad (3)$$

Ke_i and Kes_i are apparent acid dissociation constants of the enzyme and/or substrate (Ke_i), and the enzyme-substrate complex (Kes_i), and [H] is the proton concentration.[17,18] For FeMn Uf only the alkaline limb is resolved (i.e. $K_{e1} \gg K_{e2}$), thus data were fit to the following equation.

$$k_{cat}/K_m = \frac{(k_{cat}/K_m)^{max}}{(1 + Ke_2/[H])} \quad (4)$$

Stopped Flow Measurements

The reactions of native Uf and Fe^{3+}-Mn^{2+} Uf with the substrate PP were monitored at 620 nm, 25 °C, I = 0.1 M (NaCl), using an Applied Photophysics SX-18MV stopped-flow spectrophotometer. After mixing the enzyme concentration was 45 μM and substrate concentrations ranged from 3.75 mM to 50 mM. Similar to reactions previously recorded with phosphate as substrate[19,20] the time course of the absorbance change is described by a uniphasic first-order fit; corresponding k_{obs} were obtained using software provided by Applied Photophysics. In general, average k_{obs} values were obtained from five consecutive measurements.

For the analysis of the data a mechanistic model initially proposed by Sykes and coworker and recently refined Hadler *et al.* was employed (Scheme 1; see text for details).[19,21] For this scheme an equation of the type

$$k_{obs}=\frac{k_{on}A\,[S]}{B[S]^2+C\,[S]+1}+k_{off} \quad (5)$$

could be derived,[21] where k_{on} and k_{off} represent the rates for closure and opening of the μ-1,3 phosphate bridge, and A, B and C represent fitting parameters (with $A = K_{ass1}$, $B = K_{ass1}K_I$, $C = K_{ass1}(1+K_{ass2})$). While these three parameters cannot be unambiguously determined it can be shown that at high [S] equation 5 simplifies to:

$$k_{obs}=\frac{k_{on}}{K_I}\frac{1}{[S]}+k_{off} \quad (6)$$

Thus, the plot of k_{obs} *vs.* $[S]^{-1}$ is linear with the intercept corresponding to k_{off} and the slope to the ratio of k_{on}/K_I.

3. Results and Discussion

Despite considerable effort over the past decade, key aspects of the reaction mechanism employed by PAPs remain ambiguous. The identity of the active nucleophile in the hydrolysis of monoester substrates has remained obscure, not least due to the fact that the mode(s) of substrate positioning in the active site is uncertain. No crystal structure of a PAP with a bound proper substrate analogue has yet been reported. In an attempt to mimic some interactions between the enzyme and substrate several PAPs have been crystallized in presence of phosphate, the ultimate product of the PAP-catalyzed reaction. While PO_4 coordinates in μ-1,3 mode to the binuclear metal center in the active site of both pig and red kidney bean PAP,[22,23] this tetraoxo anion forms a tripodal arrangement with the metal ions in the Fe^{3+}-Mn^{2+} sweet potato PAP, whereby three of its oxygen atoms interact with the metal centers.[9] The latter observation has been interpreted in terms of the substrate binding in μ-1,3 coordination to both metal ions,[9] while the former is consistent with a mechanism whereby the substrate only binds monodentately to the divalent metal ion.[14,22,24] Similarly, metal ion replacement studies and spectroscopic studies indicate that both monodentate ligation to the divalent metal ion and metal ion-bridging bidentate coordination for the substrate are possible, and that the metal ion composition within the active site may affect the mode of coordination.[3,7-10,19]

In principle, interactions between substrates or substrate analogues with the trivalent iron can be monitored by following perturbations of the CT transition in the range 520-550 nm.[3,7-10,19,20] Sykes and coworkers demonstrated that the reaction product (and inhibitor) phosphate (P_i) rapidly binds to the divalent metal ion in Fe^{3+}-Fe^{2+} Uf, followed by a slower formation of a μ-1,3 phosphato complex, accompanied by a perturbation of the CT transition.[19] Here, we used stopped-flow measurements to monitor interactions between the substrate phenyl phosphate (PP) and Uf. Two metal ion derivatives of the enzyme were used, the native di-iron form and the Fe^{3+}-Mn^{2+} form, which also mimics the metal ion composition of a sweet potato PAP.[9,10] The Mn^{2+} derivative was used because it was shown previously that the rate of the interaction between the Fe^{3+} and P_i depends on the identity of the divalent metal ion; specifically, the substitution of Fe^{2+} by Mn^{2+} in Uf increased the rate of the CT transition perturbation (*i.e.* the rate of μ-1,3 phosphate bridge formation) approximately 12-fold.[19] In contrast, the rate for hydrolysis of the substrates *p*NPP and PP are significantly slower for the Mn^{2+}-containing derivative of Uf. Table 1 summarizes steady-state catalytic parameters

determined for the two Uf forms, including pK_a values for catalytically relevant protonation equilibria (Figure 2). While assigning pK_a values in enzymes is inherently difficult, a comparison of the pH dependence of the catalytic parameters of various metal ion derivatives of a particular protein can provide mechanistic insight. The values for pK_{e1} and pK_{e2} reflect ionizations of free enzyme and free substrate, while pK_{es1} and pK_{es2} pertain to the enzyme-substrate complex. pK_{e2} was previously assigned to the second deprotonation of the substrate *p*NPP, and pK_{es2} to a histidine residue in the second coordination sphere (His92).[9,25] pK_{e1} is only resolved in native Uf and is assigned to the deprotonation of the metal ion-bridging H_2O.[11] The assignment of pK_{es1} may depend on the metal ion composition. For native Fe^{3+}-Fe^{2+} Uf the likely protonation equilibrium corresponding for pK_{es1} is the terminal Fe^{3+}-bound H_2O/OH^-,[11] while for the Fe^{3+}-Ni^{2+} derivative pK_{es1} has been assigned to the deprotonation of the μ-hydroxide.[26] The latter is likely to be case for FeMn Uf based on the similarity of its pK_{es1} to the corresponding constant in FeMn sweet potato PAP.[9,10] The assignments of pK_{es1} to two different equilibria (*i.e.* terminal Fe^{3+}-bound H_2O/OH^- and μ-OH^-/μ-O^{2-}) were also interpreted in terms of different nucleophiles operational in these two PAPs; *i.e.* a terminal hydroxide in the diiron enzyme and a bridging (hydr)oxide in the FeNi and FeMn systems.[9-11,26] Thus, the comparative monitoring of CT perturbations by stopped-flow spectroscopy between the FeFe and FeMn forms of Uf may provide insights into alternative modes of substrate binding during hydrolysis.

The rates of perturbation (k_{obs}) observed for both the native di-iron and the FeMn Uf (Figure 3) decrease with increasing [PP] or [P_i], a trend that has also been observed for a binuclear glycerophosphodiesterase from *Enterobacter aerogenes* (GpdQ).[21] The model employed to analyze/fit the data is described in detail elsewhere.[19,21] In brief, rapid initial binding of the substrate in a catalytically non-competent mode (ES in Scheme 1) is followed by subsequent rearrangements that lead to a direct coordination of the substrate to the divalent metal ion (ES' in Scheme 1).[19,21] Binding of a second substrate molecule prevents the formation of a catalytically competent Michaelis complex, thus leading to the observed inhibition at high [S] (SES' in Scheme 1).[19,21] In this scheme k_{on} and k_{off} represent the rate constants for the closure and opening, respectively, of the μ-1,3 phosphate bridge. This bridge closure (i) can take place concomitantly with hydrolysis if a Fe^{3+}-bound terminal hydroxide acts as nucleophile (leading to the formation of a EP' complex), or (ii) precedes hydrolysis if the metal ion-bridging hydroxide is the nucleophile (i.e. the formation of a ES" complex precedes the formation of an EP complex). K_{ass1}, K_{ass2} and K_I are equilibrium constants representing binding of the substrate (K_{ass1} and K_{ass2}), and binding of an inhibitory second substrate molecule (K_I), respectively. Scheme 1 predicts mixed inhibition by phosphate and substrate inhibition at high [S]. Both of these phenomena have been documented in the closely related bovine spleen PAP.[27]

The data in Figure 3 cannot unambiguously be fit using eq. 5, however, k_{off} and the ratio k_{on}/K_I can be estimated accurately because at high substrate concentrations equation 5 can be simplified to equation 6, as described in Hadler *et al.*.[21] Hence, a plot of k_{obs} *vs.* $[S]^{-1}$ is linear with k_{off} as the intercept and the ratio k_{on}/K_I as slope. These parameters are summarized in Table 2. While K_I cannot be determined, some bounds can be estimated. The K_M of aryl phosphate substrates are ~ 1mM.[28] Binding of the inhibitory second molecule is expected to be significantly weaker than the first; this ratio has been estimated to be ~1000 for *p*NPP, and ~40 for naphthyl phosphate.[27] This leads to a range for K_I of between 0.025 and 0.001 mM^{-1}. This yields estimated bounds for k_{on} of between 1.5 s^{-1} and 0.06 s^{-1} for PP with the FeMn enzyme, and similar values for P_i. This analysis places k_{on} in a range that is considerably smaller than k_{cat} for PP (Table 1). The same conclusion holds for the FeFe form, where the estimates for k_{on} will be about an order of magnitude smaller (*i.e.* $\ll 1\ s^{-1}$).

The k_{on} and k_{off} rates are higher in the Mn derivative than in the native enzyme, independent of the substrate. It is interesting to note that the water exchange rates of $[Fe(H_2O)_6]^{2+}$ and $[Mn(H_2O)_6]^{2+}$ follow the same trend, with the Mn^{2+} complex being approximately an order of magnitude faster.[29]

The mechanistic relevance of the k_{on} values emerges from their comparison with catalytic turnover numbers for PP in Table 1. For both forms of Uf (Fe^{3+}-Fe^{2+} and Fe^{3+}-Mn^{2+}), the estimates of k_{on} with PP are considerably slower than k_{cat} (195 s^{-1} and 33 s^{-1}, respectively). This indicates that hydrolysis precedes formation of the μ-1,3 phosphate bridge and the accompanying CT perturbation. The observation that hydrolysis takes place without perturbing the Fe^{3+} site (*i.e.* hydrolysis precedes bridge closure; see above and Scheme 1) is difficult to reconcile with a mechanism that requires an Fe^{3+}-bound nucleophile. A more plausible reaction sequence thus invokes a nucleophilic water in the second coordination sphere that is deprotonated (i) by the hydroxide terminally coordinated to the Fe^{3+} as initially proposed by Averill *et al.* (ES' in Figure 4),[8] and assisted by hydrogen bonding interactions with conserved histidine residues in the substrate binding pocket (*i.e.* His92 and His195 in Scheme 2[1,3,9,14,24]). Since PP hydrolysis is more rapid than the rate of CT perturbation, it is likely that only Pi binding to the Fe^{3+} is observed experimentally, consistent with the similar k_{on} rates measured with P_i and PP (Table 2). The observed moderate rate differences are ascribed to structural variations in the active site of Uf induced via different hydrogen bond interactions between the enzyme and the respective substrate (i.e. P_i and PP). Thus, the observed on and off rates are virtually substrate-dependent, representing predominantly a post-hydrolysis equilibrium of the enzyme-Pi complex.

Conclusion

In conclusion, comparisons of the catalytic parameters with the CT perturbations in two metal ion derivatives of Uf have demonstrated that perturbations to the CT complex occur on a significantly slower timescale than catalysis. The refined reaction model that emerges from the presented work involves a rapid initial binding of the monoester substrate to the enzyme, forming a catalytically non-competent ES complex (Figure 4). In the next phase of the catalytic cycle the substrate interacts only with the divalent metal ion (ES' complex in Figure 4) and hydrolysis is initiated by a second coordination sphere nucleophilic water that is likely to be activated (i) by a hydroxide that is terminally coordinated to the Fe^{3+} and (ii) possibly also by amino acid side chains that line the substrate binding pocket (*e.g.* two conserved histidine residues as shown in Scheme 2). Following hydrolysis the M^{2+}-bound phosphate group (EP complex; Figure 4) is released and replaced by a water molecule, regenerating the active site for the next catalytic cycle. Although both k_{on} and k_{off} differ by about an order of magnitude depending on the divalent metal ion (Table 2) these differences follow the trend observed for water exchange rates (*i.e.* Mn^{2+} is more rapid than Fe^{2+}) and are thus unlikely to be of mechanistic relevance. Hence, irrespective of the identity of the divalent metal ion Uf is likely to employ a conserved mechanistic strategy whereby the M^{2+} anchors the substrate monodentately in the active site and the Fe^{3+} is essential to activate a nucleophile in the second coordination sphere. The formation of the EP' complex in Figure 4 represents thus only a post- or non-catalytic step describing the interaction between inorganic phosphate and the chromophoric metal ion in the active site.

Acknowledgments

This manuscript is dedicated to the memory of Prof. A. G. Sykes. GS, LG and AH wish to thank the ARC (DP0986292) and NIH (GM47297) for funding. We are grateful to Prof. W.W. Cleland for helpful comments.

References

(1). Sträter N, Lipscomb WN, Klabunde T, Krebs B. Angew. Chem., Int. Ed. Engl 1996;35:2025–2055.

(2). Wilcox DE. Chem. Rev 1996;96:2435–2458. [PubMed: 11848832]

(3). Mitić N, Smith SJ, Neves A, Guddat LW, Gahan LR, Schenk G. Chem. Rev 2006;106:3338–3363. [PubMed: 16895331]

(4). Cox RS, Schenk G, Mitić N, Gahan LR, Hengge AC. J. Am. Chem. Soc 2007;129:9550–9551. [PubMed: 17636903]

(5). Oddie GW, Schenk G, Angel NZ, Walsh N, Guddat LW, de Jersey J, Cassady AI, Hamilton SE, Hume DA. Bone 2000;27:575–584. [PubMed: 11062342]

(6). Bozzo GG, Raghothama KG, Plaxton WC. Biochem. J 2004;377:419–428. [PubMed: 14521509]

(7). Smoukov SK, Quaroni L, Wang X, Doan PE, Hoffman BM, Que L Jr. J. Am. Chem. Soc 2002;124:2595–2603. [PubMed: 11890810]

(8). Merkx M, Pinkse MWH, Averill BA. Biochemistry 1999;38:9914–9925. [PubMed: 10433698]

(9). Schenk G, Gahan LR, Carrington LE, Mitić N, Valizadeh M, Hamilton SE, de Jersey J, Guddat LW. Proc. Natl. Acad. Sci. USA 2005;102:273–278. [PubMed: 15625111]

(10). Mitić N, Noble CJ, Gahan LR, Hanson GR, Schenk G. J. Am. Chem. Soc 2009;131:8173–8179. [PubMed: 19507905]

(11). Smith SJ, Casellato A, Hadler KS, Mitić N, Riley MJ, Bortoluzzi AJ, Szpoganicz B, Schenk G, Neves A, Gahan LR. J. Biol. Inorg. Chem 2007;12:1207–1220. [PubMed: 17701232]

(12). Yang YS, McCormick JM, Solomon EI. J. Am. Chem. Soc 1997;119:11832–11842.

(13). Wang X, Ho RYN, Whiting AK, Que L Jr. J. Am. Chem. Soc 1999;121:9235–9236.

(14). Schenk G, Elliott TW, Leung E, Carrington LE, Mitić N, Gahan LR, Guddat LW. BMC Struct. Biol 2008;8:6. [PubMed: 18234116]

(15). Campbell HD, Dionysius DA, Keough DT, Wilson BE, de Jersey J, Zerner B. Biochem. Biophys. Res. Commun 1978;82:615–620. [PubMed: 666864]

(16). Mitić N, Valizadeh M, Leung EWW, de Jersey J, Hamilton S, Hume DA, Cassady AI, Schenk G. Arch. Biochem. Biophys 2005;439:154–164. [PubMed: 15950921]

(17). Cleland WW. Adv. Enzymol. Relat. Areas Mol. Biol 1977;45:273–387. [PubMed: 21524]

(18). Segel, IH. Enzyme kinetics : behavior and analysis of rapid equilibrium and steady state enzyme systems. Wiley; New York: 1975.

(19). Twitchett MB, Schenk G, Aquino MAS, Yiu DTY, Lau TC, Sykes AG. Inorg. Chem 2002;41:5787–5794. [PubMed: 12401084]

(20). Aquino MAS, Lim JS, Sykes AG. J. Chem. Soc., Dalton Trans 1994:429–436.

(21). Hadler K, Mitić N, Ely F, Hanson GR, Gahan LR, Larrabee JA, Ollis DL, Schenk G. J. Am. Chem. Soc 2009;131:11900–11908. [PubMed: 19653693]

(22). Klabunde T, Sträter N, Fröhlich R, Witzel H, Krebs B. J. Mol. Biol 1996;259:737–748. [PubMed: 8683579]

(23). Guddat LW, McAlpine AS, Hume D, Hamilton S, de Jersey J, Martin JL. Structure 1999;7:757–767. [PubMed: 10425678]

(24). Sträter N, Klabunde T, Tucker P, Witzel H, Krebs B. Science 1995;268:1489–1492. [PubMed: 7770774]

(25). Funhoff EG, Wang Y, Andersson G, Averill BA. FEBS J 2005;272:2968–2977. [PubMed: 15955057]

(26). Schenk G, Peralta RA, Batista SC, Bortoluzzi AJ, Szpoganicz B, Dick AK, Herrald P, Hanson GR, Szilagyi RK, Riley MJ, Gahan LR, Neves A. J. Biol. Inorg. Chem 2008;13:139–155. [PubMed: 17938975]

(27). Vincent JB, Crowder MW, Averill BA. Biochemistry 1992;31:3033–3037. [PubMed: 1372824]

(28). Valizadeh M, Schenk G, Nash K, Oddie GW, Guddat LW, Hume DA, de Jersey J, Burke TR Jr. Hamilton S. Arch. Biochem. Biophys 2004;424:154–162. [PubMed: 15047187]

(29). Helm M, Merbach AE. Coord. Chem. Rev 1999;187:151–181.

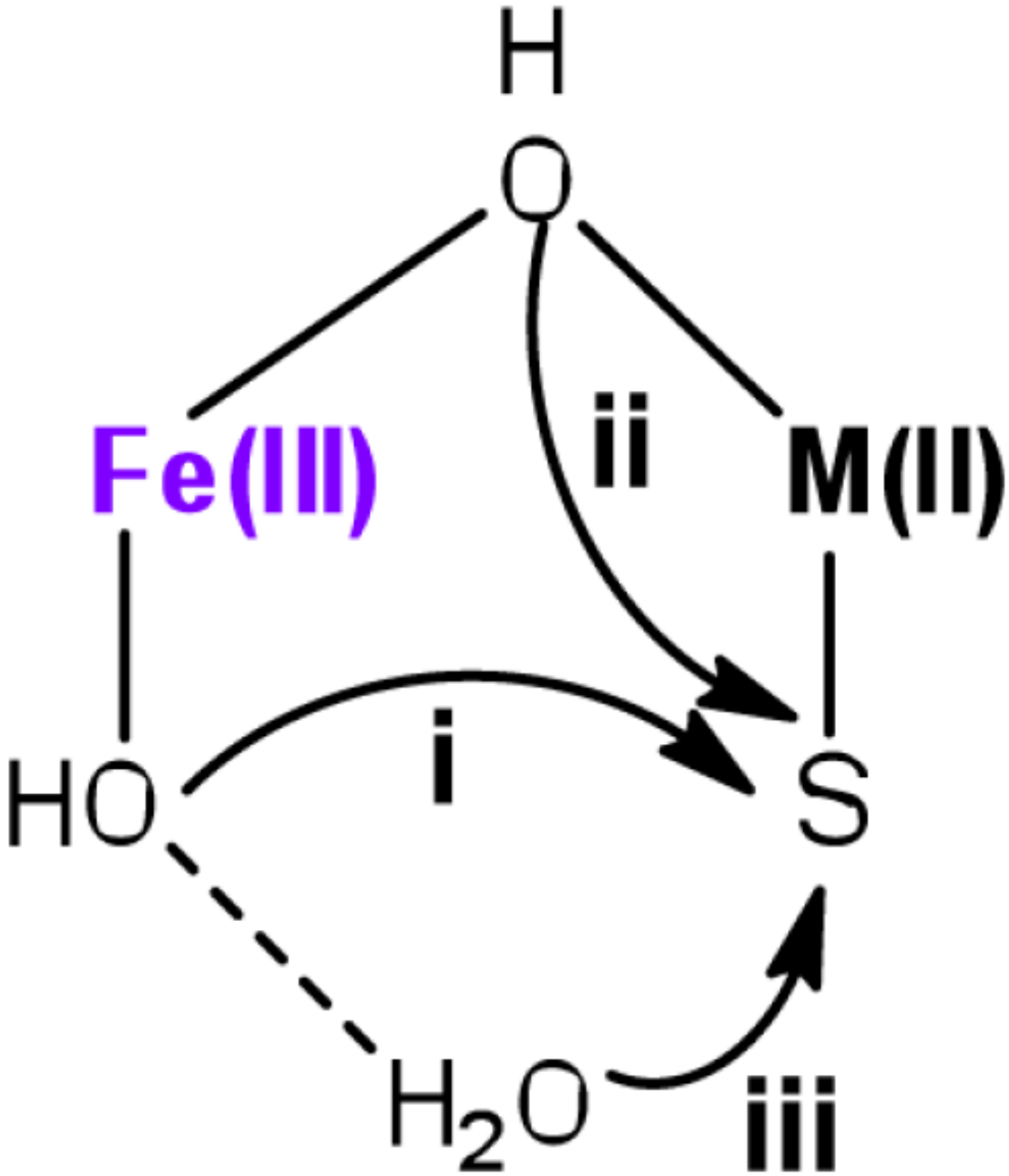

Figure 1.
Proposed nucleophilic hydroxide molecules for PAP-catalyzed hydrolysis are positioned either: (i) terminal to Fe^{3+}; (ii) bridging the two metal ions; or (iii) residing in the second coordination sphere.

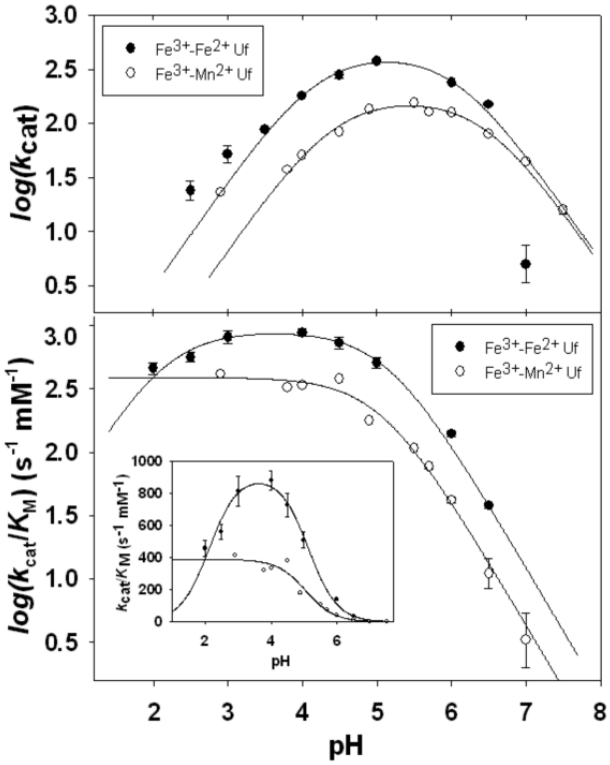

Figure 2.

Top panel: pH dependence of k_{cat} (s^{-1}) for Fe^{3+}-Fe^{2+} (filled circles) and Fe^{3+}-Mn^{2+} (open circles) Uf. Bottom panel: pH dependence of k_{cat}/K_m (s^{-1} mM^{-1}) for Fe^{3+}-Fe^{2+} (filled circles) and Fe^{3+}-Mn^{2+} (open circles) Uf. Data were measured using *p*NPP as substrate.

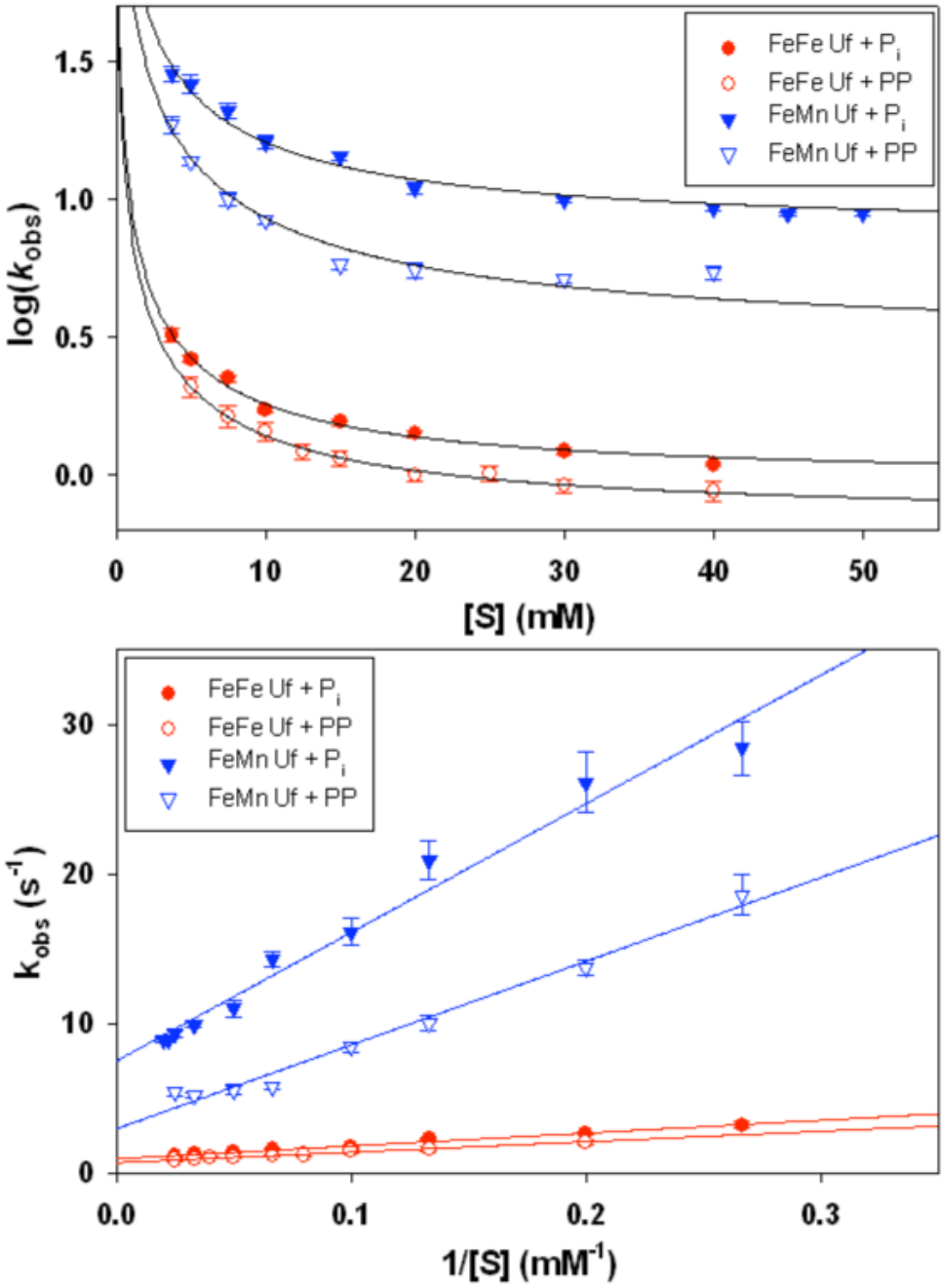

Figure 3.
First-order rate constants (k_{obs}; s^{-1}) for FeFe Uf (red) and FeMn Uf (blue) at pH 4.9, 25°C, I= 0.1 M (NaCl). Substrate concentrations ranged from 3.5 mM to 50mM. Data for P_i were reproduced from reference [7].

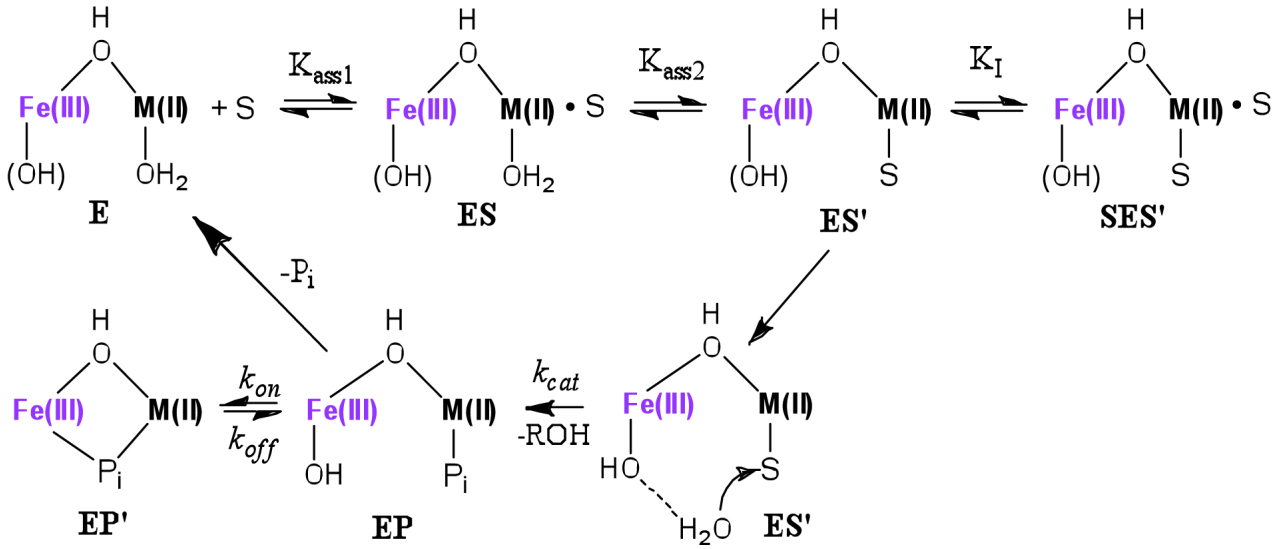

Figure 4.

Depiction of a mechanism for PAP-catalyzed substrate hydrolysis consistent with the stopped-flow kinetic data. $K_{ass}1$ and $K_{ass}2$ represent formation of first a non-competent complex, and then an ES complex in which substrate coordinates to the divalent metal ion. Binding of a second, inhibitory substrate molecule occurs with association constant K_I. Hydrolysis (k_{cat}) occurs from attack by a second-sphere nucleophilic water (see text for additional discussion). Available crystal structures show the presence of several such waters in the outer coordination sphere of the metal center. The nucleophilic water is shown in ES' in the lower part of the figure, but omitted from the upper structures for clarity.

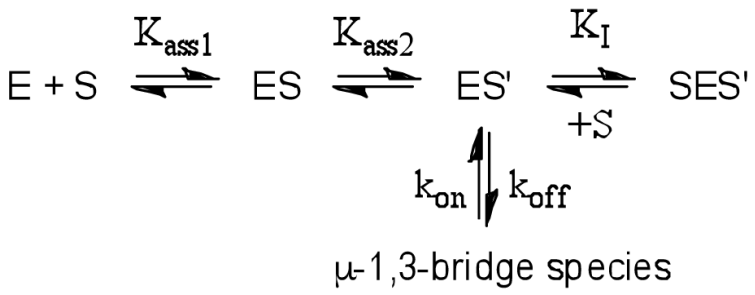

Scheme 1.

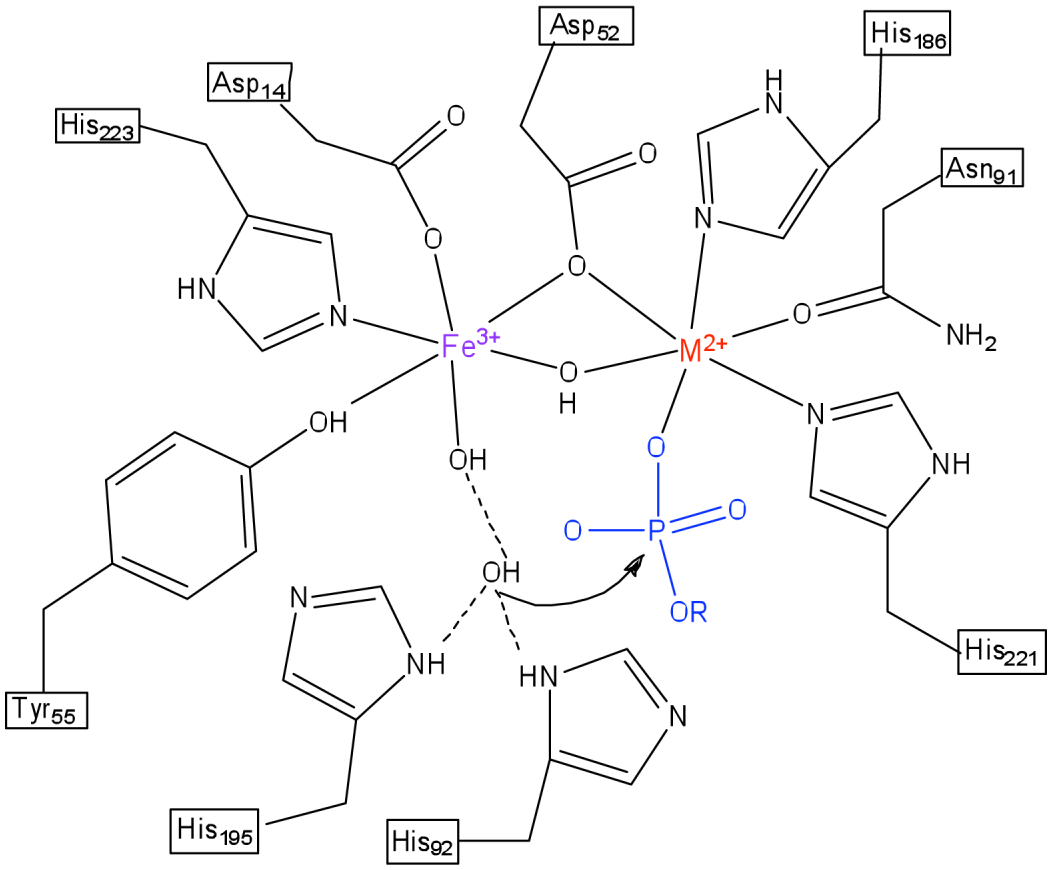

Scheme 2.
Schematic representation of the nucleophilic attack by a second coordination sphere water molecule on the phosphorus atom of the substrate.

Table 1

Kinetic data for hydrolysis of *p*NPP or PP by Uf.

Uf form	Substrate	k_{cat} (s^{-1})[a]	pK_{es1}	pK_{es2}	pK_{e1}	pK_{e2}
FeFe[b]	*p*NPP	450	4.2	6.1	2.3	4.8
FeFe	PP	195	n.d.	n.d.	n.d.	n.d.
FeMn	*p*NPP	116	4.7	6.5	-	5.1
FeMn	PP	33	n.d.	n.d.	n.d.	n.d.

n.d.: not determined.

[a] at pH 4.9

[b] from reference 28

Table 2

Fit of k_{obs} *vs.* [S] data using an equation derived for the model described in Ref. [14] (see Supplementary Information for details)

Uf form	Substrate	k_{on}/K_I (mM s^{-1})	k_{off} (s^{-1})
FeFe[7]	P_i	8.6(4)	0.94(5)
FeFe	PP	7.0(2)	0.69(2)
FeMn[7]	P_i	90(5)	7.5(6)
FeMn	PP	60(3)	3.0(4)